A DIRECT METHOD FOR CALCULATING THE THRUST AND TORQUE OF A HELICOPTER IN VERTICAL ASCENT

A THESIS

Presented to

the Faculty of the Division of Graduate Studies

Georgia School of Technology

In Partial Fulfillment

of the Requirements for the Degree

Master of Science in Aeronautical Engineering

by

Fred Blaylock Culwell, Jr.

March 1948

A DIRECT METHOD FOR CALCULATING THE THRUST
AND TORQUE OF A HELICOPTER IN VERTICAL ASCENT

Approved:

Date Approved by Chairman April 9, 1948

ACKNOWLEDGEMENTS

The author wishes to thank Mr. Walter Castles, Jr., for his suggestions and guidance on this thesis.

TABLE OF CONTENTS

Preface

Meaning of Symbols Used

Angles in Radians

α = angle of attack of a blade element at radius, r, measured between the zero lift chord line and the relative wind

χ = angle between the induced component of the inflow velocity at radius, r, and the normal to the rotor

θ_r = angle of incidence of a blade element at radius, r, measured between the zero lift chord line and the plane of rotation

φ = induced angle of attack of a blade element at radius, r, measured between the relative wind and the plane of rotation

Areas

$dA = 2\pi r\,dr$ = area of an elemental rotor annulus

$A = \pi R^2$ = rotor disk area

Forces

dL = lift on an elemental rotor annulus

dT = thrust on an elemental rotor annulus

T = rotor thrust

Lengths

C_r = chord of a blade element at radius, r

r = distance of a blade element from the axis of rotation

R = rotor radius

Miscellaneous

a_o = slope of the lift curve of a blade element

= C_ℓ/radian

dM' = mass flow through an elemental annulus

Ω = angular velocity of the rotor in radians/second

ρ = mass density of air

Moments

dQ = torque about the rotor axis of rotation of the air forces on an elemental annulus

Q = rotor torque about the axis of rotation of the air forces

Nondimensional Coefficients

C_D = rotor blade element drag coefficient

C_{D_o} = profile drag coefficient of a blade element

C_{D_i} = inflow drag coefficient of a blade element

C_{ℓ_r} = lift coefficient at a blade element at radius, r

dC_Q = rotor torque coefficient about the axis of rotation of air forces on an elemental annulus

$C_Q = \dfrac{Q}{\rho \pi \Omega^2 R^5}$ = rotor torque coefficient

dC_T = rotor thrust coefficient of air forces on an elemental rotor annulus

$C_T = \dfrac{T}{\rho \pi \Omega^2 R^4}$ = rotor thrust coefficient

Nondimensional Parameters

b = number of rotor blades

k_u = factor to account for the total head loss above the annulus due to the effects of viscosity

k_l = factor to account for the total head loss below the annulus due to the effects of viscosity

k_1 = weighted mean value of k_l across the rotor

$\sigma_r = \frac{bc_r}{\pi r}$ = rotor solidity at radius, r

$\lambda_v = \frac{V_v}{V_o}$ = ratio of the vertical ascent velocity to the induced velocity in hovering flight of an actuator disk with the given thrust

$\lambda = \frac{V_v}{\Omega R}$ = ratio of the vertical ascent velocity to the rotor blade tip velocity

Pressure

H = total head

P_o = atmospheric pressure

P_1 = static pressure just above the rotor annulus

P_2 = static pressure just below the rotor annulus

Velocities

V_i = induced velocity at a blade element at radius, r

V_∞ = resultant induced velocity at a large distance below the rotor annulus where the streamlines are normal to the rotor plane

V_v = velocity at which the rotor is ascending vertically

ΔV = total change in velocity along the line of thrust of the air in any elemental stream tube

$V_o = \sqrt{\frac{T}{2\rho A}}$ = value of the induced velocity for an actuator disk in hovering flight

A Direct Method for Calculating the Thrust and Torque of a Helicopter in Vertical Ascent

I Summary

The object of this investigation is to find a more convenient and sufficiently exact method for calculating the thrust and torque of a helicopter rotor in vertical ascent.

Equations for the general case of rotors having blades with any twist and taper are derived by a combination of the momentum and blade element theories. A semi-empirical constant, k_1, which corrects for the effects of viscosity is introduced. Several simplifying approximations are made in order to obtain a direct solution.

The thrust and torque coefficients are calculated from the theory for a particular model rotor on which test data was available. The results are satisfactory for the special case of hovering flight and at low rates of vertical ascent, but for higher rates of vertical ascent the theoretical values of the thrust coefficients are progressively higher than the experimental values. The theoretical torque coefficient values are in good agreement with the experimental values over the whole range.

II Introduction

Very little work has been done on predicting the thrust and torque characteristics of a helicopter rotor in vertical ascent. Glauert[1] derived a theory for the analysis of helicopter rotor performance in vertical ascent by the use of the vortex theory. This theory, with certain modifications, was used by Fagan[2] for the performance calculations of a lifting airscrew in vertical ascent. The calculations are very involved and the results did not check well enough with the existing experimental data to warrant this application of the vortex theory in computing the thrust and torque characteristics.

Thus, there is a need for a more accurate and less involved method for calculating the thrust and torque of a helicopter rotor in vertical ascent. In this paper the induced velocity at a given radius, r, is set up as a function of the thrust at that radius and the rate of ascent. An empirical constant is introduced to account for the effects of viscosity.

---

[1]Herman Glauert, On the Vertical Ascent of a Helicopter, (Aeronautical Research Committee, Reports and Memoranda, No. 1132, 1927), p. 360

[2]Robert H. Fagan, Vertical Ascent Analysis of the Lifting Airscrew, (unpublished Master's thesis, Georgia School of Technology, 1940)

III Theory

The streamlines which pass through the circumference of a circle about the axis of symmetry of the flow form a surface which, for the flow under consideration, is a stream tube. The cross sectional area between two adjacent stream tubes at the plane of rotation of a rotor defines a rotor annulus of radius, r, and width, dr.

In writing Bernoulli's equation, $H = P + \frac{\rho}{2} V^2$, between any two points along a stream tube it is assumed that there is no loss of energy for a perfect fluid. However, in a real fluid there is a change in energy due to viscosity. The velocity distribution at the rotor is non-uniform, but at a great distance below the rotor the velocity distribution tends to become uniform,[3] so there will be an exchange in energy between the adjacent stream tubes. A viscosity correction factor is introduced in Bernoulli's equation to account for the change in energy.

It is first assumed that the coordinates are fixed in space. Then as shown in Figure (1), at some point (1) a great distance above the rotor annulus, the pressure is the atmospheric value, P_o , and the velocity is zero. Just above the rotor at point (2) the pressure is P_1 and the velocity is V_i , where P_1 = static pressure and V_i = induced velocity. At a point (3), just below the rotor, the static pressure is P_2 and the velocity is also V_i . At point (4), a great distance below the rotor, the static pressure is again equal to the atmospheric pressure, P_o , and the velocity is V_∞ where V_∞ = resultant induced velocity at a large distance below the rotor annulus where the streamlines are normal to the rotor plane.

---

[3] W. F. Durand, Aerodynamic Theory, (Berlin: Julius Springer, 1935. Vol. III), p. 162

The pressure loss above the rotor is a function of the induced velocity, $f(V_i^2)$, and that below the rotor, $f(V_\infty^2)$. Putting in the factor to account for the change in energy between the adjacent stream tubes due to viscosity, the dynamic pressure terms above and below the rotor become, respectively, $\frac{\rho}{2} k_u V_i^2$ and $\frac{\rho}{2} k_l V_\infty^2$

where

k_u = factor to account for the total head loss above the annulus due to the effects of viscosity

k_l = factor to account for the total head loss below the annulus due to the effects of viscosity

Assuming now that the coordinates are moving with the rotor, the relative velocity between the rotor and the free stream is the rate of vertical ascent as can be seen from Figure (2). A point (1) is selected at a very great distance above the rotor where the static pressure is equal to the atmospheric pressure, P_o , and the velocity is V_v , the velocity at which the rotor is ascending vertically. At point (2), just above the rotor, the static pressure is P_1 and the velocity is $(V_v + V_i)$. Bernoulli's equation is written between points (1) and (2) as

$$P_o + \frac{\rho}{2} V_v^2 = P_1 + \frac{\rho}{2} (V_v + V_i)^2 \qquad (1)$$

or by expanding the dynamic pressure terms and introducing the viscosity correction factor, equation (1) becomes

$$P_o = P_1 + \frac{\rho}{2} (V_v^2 + 2 V_v V_i + k_u V_i^2) - \frac{\rho}{2} V_v^2 \qquad (2)$$

Bernoulli's equation can not be written between a point above the rotor and another point below the rotor, because there is a discontinuity on the pressure field at the rotor.

At a point (3), just below the rotor, the static pressure is P_2 and the velocity is $(V_r + V_i)$. At point (4), a great distance below the rotor, the static pressure is again equal to the atmospheric pressure, P_o and the velocity is $(V_r + V_\infty)$. Applying Bernoulli's equation between these two points gives

$$P_2 + \frac{\rho}{2}(V_r + V_i)^2 = P_o + \frac{\rho}{2}(V_r + V_\infty)^2 \qquad (3)$$

and again by expanding the dynamic pressure terms and including the viscosity correction factor, equation (4) becomes

$$P_o = P_2 + \frac{\rho}{2}(V_r^2 + 2V_r V_i + V_i^2) - \frac{\rho}{2}(V_r^2 + 2V_r V_\infty + k_l V_\infty^2) \qquad (4)$$

Combining equations (2) and (4) gives

$$P_1 + \frac{\rho}{2}V_r^2 + \rho V_r V_i + \frac{\rho}{2}k_m V_i^2 - \frac{\rho}{2}V_r^2 = P_2 + \frac{\rho}{2}V_r^2 + \rho V_r V_i + \frac{\rho}{2}V_i^2 - \frac{\rho}{2}V_r^2 - \rho V_r V_\infty - \frac{\rho}{2}k_l V_\infty^2 \qquad (5)$$

or

$$P_2 - P_1 = \frac{\rho}{2}V_i^2(k_m - 1) + \frac{\rho}{2}V_\infty(2V_r + k_l V_\infty) \qquad (6)$$

According to the propeller momentum theory[4], approximately three-fourths of the dynamic pressure change takes place below the rotor for a perfect fluid with no viscosity or compressibility effects. The approximation is made that the total head loss due to viscosity above the rotor is small compared to the loss below the rotor. Then $k_m = 1$, and equation (6) can now be written as

---

[4] W. J. M. Rankine, On the Mechanical Principles of the Action of Propellers, (Trans. Inst. Naval Architects, 1865), p. 13

$$P_2 - P_1 = \frac{\rho}{2} V_\infty (2V_r + k_u V_\infty) \tag{7}$$

The thrust acting on the annulus is equal to the difference in static pressures above and below the annulus multiplied by the annulus area or

$$dT = (P_2 - P_1)\, dA \tag{8}$$

where

dT = thrust on an elemental rotor annulus

$dA = 2\pi r\, dr$ = area of an elemental rotor annulus

The mass flow through an elemental annulus can be written as

$$dM' = \rho(V_r + V_i \cos\chi)\, dA \tag{9}$$

where

ρ = mass density of air

χ = angle between the induced component of the inflow velocity at radius, r, and the normal to the rotor

$V_i \cos\chi$ = component of the induced velocity normal to the rotor

The thrust acting on an elemental annulus is equal to the rate of change of momentum along the line of thrust of the air passing through the annulus. Thus

$$dT = dM' \Delta V = \rho(V_r + V_i \cos\chi)\, dA\, V_\infty \tag{10}$$

where

ΔV = total change in velocity along the line of thrust of the air in any elemental stream tube

$= V_\infty$

Combining equations (8) and (10) gives

$$(P_2 - P_1)\, dA = \rho\,(V_v + V_i \cos\chi)\, dA\, V_\infty \tag{11}$$

Substituting the value of $(P_2 - P_1)$ of equation (7) into equation (11) gives

$$\frac{\rho}{2}(2V_v + k_l V_\infty) V_\infty\, dA = \rho\,(V_v + V_i \cos\chi)\, V_\infty\, dA \tag{12}$$

and cancelling out ρ, dA, and V_∞ from both sides of the equation,

$$V_v + V_i \cos\chi = V_v + \frac{k_l V_\infty}{2} \tag{13}$$

or

$$V_\infty = \frac{2 V_i \cos\chi}{k_l} \tag{14}$$

Substituting the value of V_∞ from equation (14) into equation (10) gives

$$dT = \rho\,(V_v + V_i \cos\chi)\,\frac{2 V_i \cos\chi}{k_l}\, dA \tag{15}$$

or since $dA = 2\pi r\, dr$

$$dT = \frac{4\pi\rho V_i}{k_l}\,(V_v + V_i \cos\chi)\, V_i \cos\chi\, r\, dr \tag{16}$$

The value of k_l will vary across the rotor. Defining k_1 as the weighted mean value of k_l, equation (16) becomes

$$dT = \frac{4\pi\rho V_i}{k_1}\,(V_v + V_i \cos\chi)\, V_i \cos\chi\, r\, dr \tag{17}$$

The total thrust acting on the blade element is the vector sum of the components of the lift and profile drag acting in the vertical direction. Since the component due to the profile drag is very small compared to the component of the lift (see Figure (3)) it may be neglected. The thrust equation is then written as

$$dT = \frac{\rho}{2}\, b C_r V^2 C_{l_r} \cos\phi\, dr \tag{18}$$

where

b = number of rotor blades

C_r = chord of a blade element at radius, r

C_{lr} = lift coefficient at a blade element at radius, r

ϕ = induced angle of attack of a blade element at radius, r, measured between the relative wind and the plane of rotation

$V_i \cos \chi$ is small compared to V_v for large rates of vertical ascent as shown in Figure (3). For small rates of vertical ascent $V_i \cos \chi$ is small compared to Ωr, over the outer portion of the blades where the forces are large. Therefore, the following approximations are made:

(1) $$V = \sqrt{V_v^2 + \Omega^2 r^2}$$

(2) $$\cos \phi = \frac{\Omega r}{V} = \frac{\Omega r}{\sqrt{V_v^2 + \Omega^2 r^2}}$$

(3) $$\sin \phi = \frac{V_v + V_i \cos \chi}{V} = \frac{V_v + V_i \cos \chi}{\sqrt{V_v^2 + \Omega^2 r^2}}$$

where

Ω = angular velocity of the rotor in radians/second

Substituting the values of V and $\cos \phi$ of approximations (1) and (2) into equation (18) gives

$$dT = \frac{\rho}{2} b C_r (V_v^2 + \Omega^2 r^2) C_{lr} \frac{\Omega r}{(V_v^2 + \Omega^2 r^2)^{1/2}} dr \qquad (19)$$

or

$$dT = \frac{\rho}{2} b C_r (V_v^2 + \Omega^2 r^2)^{1/2} C_{lr} \Omega r \, dr \qquad (20)$$

Equating the values of thrust, dT, of equations (17) and (20) gives

$$\frac{4\pi\rho}{k_1}(V_v + V_i\cos\chi)V_i\cos\chi\, r\,dr = \frac{\rho}{2} b C_r (V_v^2 + \Omega^2 r^2)^{1/2} C_{l_r}\Omega r\,dr \qquad (21)$$

Upon simplification equation (21) becomes

$$V_i^2\cos^2\chi + V_v V_i\cos\chi - \frac{k_1 b C_r}{8\pi}(V_v^2 + \Omega^2 r^2)^{1/2} C_{l_r}\Omega = 0 \qquad (22)$$

Substituting the value of $\sigma_r = \frac{bC_r}{\pi r}$ in equation (22) gives

$$V_i^2\cos^2\chi + V_v V_i\cos\chi - \frac{k_1\sigma_r C_{l_r}}{8}(V_v^2 + \Omega^2 r^2)^{1/2}\Omega r = 0 \qquad (23)$$

where

σ_r = rotor solidity at radius, r

Solving equation (23) for $V_i\cos\chi$

$$V_i\cos\chi = -\frac{V_v}{2} \pm \sqrt{\left(\frac{V_v}{2}\right)^2 + \frac{k_1\sigma_r C_{l_r}}{8}(V_v^2 + \Omega^2 r^2)^{1/2}\Omega r} \qquad (24)$$

The sign in front of the radical is positive because the value of $V_i\cos\chi$ in hovering flight, when $V_v = 0$, is equal to $+\sqrt{\frac{k_1\sigma_r C_{l_r}\Omega^2 r^2}{8}}$

The torque loading in ft.#/ft.^{2} of a helicopter rotor is relatively small compared to that of a propeller. The induced rotation of the airstream is, therefore, small enough to be neglected. Thus the angle φ is written with sufficient accuracy as

$$\varphi = TAN^{-1}\frac{(V_v + V_i\cos\chi)}{\Omega r} \qquad (25)$$

where

φ = inflow angle of a blade element at radius, r, measured between the relative wind and the plane of rotation

Substituting the value of $V_i\cos\chi$ of equation (24) into equation (25) gives

$$\varphi = TAN^{-1}\left[\frac{V_V}{\Omega r} - \frac{V_V}{2\Omega r} + \sqrt{\left(\frac{V_V}{2\Omega r}\right)^2 + \frac{k_1 \sigma_r C_{\ell r}}{8}\left[\left(\frac{V_V}{\Omega r}\right)^2 + 1\right]^{1/2}}\right] \tag{26}$$

Letting $\lambda = \frac{V_V}{\Omega R}$, equation (26) becomes

$$\varphi = TAN^{-1}\left[\frac{\lambda R}{2r} + \sqrt{\left(\frac{\lambda R}{2r}\right)^2 + \frac{k_1 \sigma_r C_{\ell r}}{8}\left[\left(\frac{\lambda R}{r}\right)^2 + 1\right]^{1/2}}\right] \tag{27}$$

From Figure (3) it can be seen that

$$\varphi = \theta_r - \alpha = \theta_r - \frac{C_{\ell r}}{a_0} \tag{28}$$

where

θ_r = angle of incidence of a blade element at radius, r, measured between the zero lift chord line and the plane of rotation

α = angle of attack of a blade element at radius, r, measured between the zero lift chord line and the relative wind

a_0 = slope of the lift curve of a blade element

Equation (28) is rearranged so that

$$\frac{C_{\ell r}}{a_0} = \theta_r - \varphi \tag{29}$$

Substituting the value of φ from equation (27) into equation (29) gives

$$\frac{C_{\ell r}}{a_0} = \theta_r - TAN^{-1}\left[\frac{\lambda R}{2r} + \sqrt{\left(\frac{\lambda R}{2r}\right)^2 + \frac{k_1 \sigma_r C_{\ell r}}{8}\left[\left(\frac{\lambda R}{r}\right)^2 + 1\right]^{1/2}}\right] \tag{30}$$

For any given values of θ_r , a_0 , λ , k_1 , σ_r and R/r, equation (30) can be solved for $C_{\ell r}$.

From equation (20) the rotor thrust is written as

$$T = \int_0^R \frac{\rho}{2} b C_r (V_V^2 + \Omega^2 r^2) C_{\ell r}^{1/2} \Omega r \, dr \tag{31}$$

In terms of $\sigma_r = \frac{bC_r}{\pi r}$ and $\lambda = \frac{V_v}{\Omega R}$ equation (31) becomes

$$T = \int_0^R \frac{\rho}{2} \frac{bC_r}{\pi r} \pi r \left(\frac{V_v^2}{\Omega^2 r^2} \frac{R^2}{R^2} + 1 \right)^{1/2} C_{l_r} \Omega^2 r^2 \, dr \tag{32}$$

or

$$T = \int_0^R \frac{\rho}{2} \pi \Omega^2 \sigma_r \left[\left(\frac{\lambda R}{r} \right)^2 + 1 \right]^{1/2} C_{l_r} \, r^3 \, dr \tag{33}$$

Both sides of equation (33) are divided by $\rho \pi \Omega^2 R^4$ so

$$\frac{T}{\rho \pi \Omega^2 R^4} = \frac{\rho \pi \Omega^2}{2 \rho \pi \Omega^2 R^4} \int_0^R \sigma_r \left[\left(\frac{\lambda R}{r} \right)^2 + 1 \right]^{1/2} C_{l_r} \, r^3 \, dr \tag{34}$$

By definition $C_T = \frac{T}{\rho \pi \Omega^2 R^4}$ so equation (34) becomes

$$C_T = \int_0^R \frac{\sigma_r}{2} \left[\left(\frac{\lambda R}{r} \right)^2 + 1 \right]^{1/2} C_{l_r} \frac{r^3}{R^4} \, dr \tag{35}$$

Expressing the elemental radius as a fraction of the rotor radius, i.e., r/R, the integral of equation (35) becomes

$$C_T = \int_0^1 \frac{\sigma_r}{2} \left[\left(\frac{\lambda R}{r} \right)^2 + 1 \right]^{1/2} C_{l_r} \left(\frac{r}{R} \right)^3 d\left(\frac{r}{R} \right) \tag{36}$$

The integration in the above equation for the rotor thrust coefficient is most easily performed graphically.

The torque of the drag forces on the blade elements lying within the annulus is

$$dQ = \frac{\rho}{2} b C_r V^2 C_D \, r \, dr \tag{37}$$

where

dQ = torque about the rotor axis of rotation of air forces on an elemental annulus

C_D = rotor blade element drag coefficient

The drag is broken up into components as can be seen in Figure (3) so that

equation (37) is written

$$dQ = \frac{\rho}{2} b C_r V^2 (C_{D_0} \cos\phi + C_{l_r} \sin\phi) r\, dr \tag{38}$$

or

$$dQ = \frac{\rho}{2} b C_r V^2 C_{D_0} \cos\phi\, r\, dr + \frac{\rho}{2} b C_r V^2 C_{l_r} \sin\phi\, r\, dr \tag{39}$$

where

C_{D_0} = profile drag coefficient of a blade element operating at a lift coefficient, C_{l_r}

Substituting the values of V, $\cos\phi$, and $\sin\phi$ of approximations (1), (2) and (3) into equation (39) gives

$$dQ = \frac{\rho}{2} b C_r (V_v^2 + \Omega^2 r^2) C_{D_0} \frac{\Omega r}{(V_v^2 + \Omega^2 r^2)^{1/2}} r\, dr$$
$$+ \frac{\rho}{2} b C_r (V_v^2 + \Omega^2 r^2) C_{l_r} \frac{(V_v + v_i \cos\chi)}{(V_v^2 + \Omega^2 r^2)^{1/2}} r\, dr \tag{40}$$

The value of $v_i \cos\chi$ of equation (24) is substituted in equation (40) which then reduces to

$$dQ = \frac{\rho}{2} b C_r (V_v^2 + \Omega^2 r^2)^{1/2} C_{D_0} \Omega r^2 dr$$
$$+ \frac{\rho}{2} b C_r (V_v^2 + \Omega^2 r^2) C_{l_r} \left[\frac{\frac{V_v}{2} + \sqrt{\left(\frac{V_v}{2}\right)^2 + \frac{k_1 \sigma_r C_{l_r} (V_v^2 + \Omega^2 r^2)^{1/2} \Omega r}{8}}}{(V_v^2 + \Omega^2 r^2)^{1/2}} \right] r\, dr \tag{41}$$

or

$$dQ = \frac{\rho}{2} b C_r (V_v^2 + \Omega^2 r^2)^{1/2} C_{D_0} \Omega r^2 dr + \frac{\rho}{4} V_v b C_r (V_v^2 + \Omega^2 r^2)^{1/2} C_{l_r} r\, dr$$
$$+ \frac{\rho}{2} b C_r (V_v^2 + \Omega^2 r^2)^{1/2} C_{l_r} \left[\sqrt{\left(\frac{V_v}{2}\right)^2 + \frac{k_1 \sigma_r C_{l_r} (V_v^2 + \Omega^2 r^2)^{1/2} \Omega r}{8}} \right] r\, dr \tag{42}$$

Equation (42) can be expressed in terms of $\sigma_r = \frac{b C_r}{\pi r}$ and $\lambda = \frac{V_v}{\Omega R}$ as

$$dQ = \frac{\pi r}{\pi r}\frac{\rho}{2} b C_r \left[\frac{V_v^2}{\Omega^2 r^2}\frac{R^2}{R^2} + 1\right]^{1/2} \Omega^2 C_{D_0} r^3 dr$$

$$+ \frac{\pi r}{\pi r}\frac{\rho}{4} b C_r V_v \frac{\Omega R}{\Omega R}\left[\frac{V_v^2}{\Omega^2 r^2}\frac{R^2}{R^2} + 1\right]^{1/2} \Omega C_{l_r} r^2 dr$$

$$+ \frac{\pi r}{\pi r}\frac{\rho}{2} b C_r \left[\frac{V_v^2}{\Omega^2 r^2}\frac{R^2}{R^2} + 1\right]^{1/2} \Omega r C_{l_r}\left[\Omega r \sqrt{\frac{V_v^2}{4\Omega^2 r^2}\frac{R^2}{R^2} + \frac{k_1 \sigma_r C_{l_r}}{8}\left[\frac{V_v^2}{\Omega^2 r^2}\frac{R^2}{R^2} + 1\right]^{1/2}}\right] r dr \quad (43)$$

or

$$dQ = \frac{\rho}{2}\pi \Omega^2 \sigma_r \left[\left(\frac{\lambda R}{r}\right)^2 + 1\right]^{1/2} C_{D_0} r^4 dr$$

$$+ \frac{\rho}{4}\pi \Omega^2 \sigma_r \left[\left(\frac{\lambda R}{r}\right)^2 + 1\right]^{1/2} \lambda R C_{l_r} r^3 dr$$

$$+ \frac{\rho}{2}\pi \Omega^2 \sigma_r \left[\left(\frac{\lambda R}{r}\right)^2 + 1\right]^{1/2} C_{l_r}\left[\sqrt{\left(\frac{\lambda R}{2r}\right)^2 + \frac{k_1 \sigma_r C_{l_r}}{8}\left[\left(\frac{\lambda R}{r}\right)^2 + 1\right]^{1/2}}\right] r^4 dr \quad (44)$$

The equation for the rotor torque about the axis of rotation due to the air forces is written as

$$Q = \frac{\rho}{2}\pi \Omega^2 \int_0^R \sigma_r \left[\left(\frac{\lambda R}{r}\right)^2 + 1\right]^{1/2} C_{D_0} r^4 dr$$

$$+ \frac{\rho}{4}\pi \lambda R \Omega^2 \int_0^R \sigma_r \left[\left(\frac{\lambda R}{r}\right)^2 + 1\right]^{1/2} C_{l_r} r^3 dr$$

$$+ \frac{\rho}{2}\pi \Omega^2 \int_0^R \sigma_r \left[\left(\frac{\lambda R}{r}\right)^2 + 1\right]^{1/2} C_{l_r}\left[\sqrt{\left(\frac{\lambda R}{2r}\right)^2 + \frac{k_1 \sigma_r C_{l_r}}{8}\left[\left(\frac{\lambda R}{r}\right)^2 + 1\right]^{1/2}}\right] r^4 dr \quad (45)$$

By definition $C_Q = \frac{Q}{\rho \pi \Omega^2 R^5}$, so dividing both sides of equation (45) by $\rho \pi \Omega^2 R^5$ gives

$$C_Q = \frac{1}{2}\int_0^R \sigma_r \left[\left(\frac{\lambda R}{r}\right)^2 + 1\right]^{1/2} C_{D_0} \frac{r^4}{R^5}\, dr + \frac{\lambda}{4}\int_0^R \sigma_r \left[\left(\frac{\lambda R}{r}\right)^2 + 1\right]^{1/2} C_{l_r} \frac{r^3}{R^4}\, dr$$

$$+ \frac{1}{2}\int_0^R \sigma_r \left[\left(\frac{\lambda R}{r}\right)^2 + 1\right]^{1/2} C_{l_r} \left[\sqrt{\left(\frac{\lambda R}{2r}\right)^2 + \frac{k_1 \sigma_r C_{l_r}}{8}\left[\left(\frac{\lambda R}{r}\right)^2 + 1\right]^{1/2}}\right] \frac{r^4}{R^5}\, dr \qquad (46)$$

Expressing the elemental radius as a fraction of the rotor radius, i.e., r/R, the integrals of equation (46) become

$$C_Q = \frac{1}{2}\int_0^1 \sigma_r \left[\left(\frac{\lambda R}{r}\right)^2 + 1\right]^{1/2} C_{D_0} \left(\frac{r}{R}\right)^4 d\left(\frac{r}{R}\right) + \frac{\lambda}{4}\int_0^1 \sigma_r \left[\left(\frac{\lambda R}{r}\right)^2 + 1\right]^{1/2} C_{l_r} \left(\frac{r}{R}\right)^3 d\left(\frac{r}{R}\right)$$

$$+ \frac{1}{2}\int_0^1 \sigma_r \left[\left(\frac{\lambda R}{r}\right)^2 + 1\right]^{1/2} C_{l_r} \left[\sqrt{\left(\frac{\lambda R}{2r}\right)^2 + \frac{k_1 \sigma_r C_{l_r}}{8}\left[\left(\frac{\lambda R}{r}\right)^2 + 1\right]^{1/2}}\right] \left(\frac{r}{R}\right)^4 d\left(\frac{r}{R}\right) \qquad (47)$$

These integrals are easily integrated by graphical integration in calculating the rotor torque coefficients.

IV Procedure

In order to make the thrust and torque coefficient calculations less laborous, a plot of equation (30) is shown on Figure (4) for the positive values of the lift coefficients at radius, r, and on Figure (5) for the negative lift coefficients. These plots afford a graphical trial and error solution of equation (30).

For a particular rate of vertical ascent, V_v, and a given value of C_T, the corresponding value of λ_v is obtained as follows:

$$\lambda_v = \frac{V_v}{V_o} \qquad \text{by definition}$$

where

V_v = rate of vertical ascent

$$V_o = \sqrt{\frac{T}{2\rho A}}$$

$$\lambda_v = \frac{V_v}{\sqrt{\frac{T}{2\rho A}}} = \frac{V_v}{\sqrt{\frac{\rho \pi \Omega^2 R^4 C_T}{2\rho \pi R^2}}} \tag{48}$$

where

$$T = \rho \pi \Omega^2 R^4 C_T \qquad \text{and} \qquad A = \pi R^2$$

Then

$$\lambda_v = \frac{V_v}{\Omega R \sqrt{\frac{C_T}{2}}} \qquad\qquad \lambda = \frac{V_v}{\Omega R}$$

or finally

$$\lambda_v = \frac{\lambda}{\sqrt{\frac{C_T}{2}}} \tag{49}$$

The value of k, corresponding to the calculated value of λ_v is obtained from Figure (6).

Glauert[5] developed a semi-empirical curve relating the inflow velocity to the rate of descent for the case of a propeller in the vortex ring state. This relation accounted for the effects of viscosity. According to Glauert's curve, the viscosity correction factor becomes zero for relatively small rates of vertical ascent.

For this paper the approximation is made that the values of k_1, of Figure (6) are the reciprocal of the contraction ratio. The value for k_1, of approximately $\sqrt{2}$ for hovering flight has previously been substantiated by experimental data.

Knowing θ_r, a_o, λ, and k_1, equation (30) can be solved for C_{l_r}, the lift coefficient at any radius, r. For the calculation of C_T and C_Q it is assumed that the value of the slope of the lift curve, a_o, is 2π/radian. For a cascade of thin two dimensional airfoils, perfect fluid theory predicts a slope slightly greater than 2π/radian[6]. The effects of viscosity reduce this value to about 5.75/radian for the case of a thin two dimensional airfoil in a real fluid. As the effects of viscosity are corrected for in this paper by a factor, k_1, it is felt that the use of a slope of 2π/radian is reasonable.

The graph on Figure (4) is divided into four quadrants. To use this graph for the solution of equation (30), an arbitrary positive value of C_{l_r}/β is selected. The lower left quadrant is a plot of C_{l_r}/β vs. $k_1 \sigma_r C_{l_r}/\beta$ for different values of $k_1 \sigma_r$. At any radius, r, the value of $\sigma_r = \frac{bC_r}{\pi r}$ is calculated and knowing k_1, the value of $k_1 \sigma_r C_{l_r}/\beta$

---

[5] Durand, op. cit., p. 350, Vol. IV

[6] Ibid., p. 230

can be obtained from the graph.

The upper left quadrant is a plot of $k, \sigma_r C_{lr}/\beta$ vs. ϕ for different values of $\lambda R/r$. From the value of $k, \sigma_r C_{lr}/\beta$ determined in the lower quadrant and the known value of vertical ascent, λ, the value of ϕ can be found.

The upper right quadrant contains a plot of ϕ vs. C_{lr}/a_o, for different values of θ_r. Using the value found for ϕ and an assumed value of θ_r, the value of C_{lr}/a_o is determined.

The lower right quadrant is a plot of C_{lr}/a_o vs. C_{lr}/β with the slanting lines joining equal values of C_{lr}.

The method of solution is to select positive values of C_{lr}/β and trace through the graph as explained until the value of C_{lr}/β at the end of the trial corresponds to the assumed value at the beginning of the trial. This procedure will yield the value of C_{lr} at any particular radius, r, at which the elemental lift coefficient is positive.

At some inboard radius along the rotor blade, the lift coefficient may become negative. Coming inboard along the radius from the rotor blade tip the value of C_{lr} becomes increasingly small and at some radius becomes zero. Beyond this radius the positive graph (Figure (4)) yields no solution so the negative graph (Figure (5)) is used with the same procedure as for the positive graph to yield the negative values of C_{lr}.

Values of C_{lr} must be determined at a sufficient number of stations along the rotor blade in order that the thrust and torque coefficients can be calculated.

At some radius along the rotor blade near the axis of rotation, the radical term in equation (30) may become imaginary, thus no solution from

Figure (4) or (5) can be obtained. This indicates that there is a vortex ring in the flow at that point and the equations derived in this paper are not valid. The thrust and torque at the axis of rotation are zero so the approximation is made that the curves of dC_T and dC_Q vs. (r/R) are faired in from a point on the curves where equation (30) becomes imiginary to zero at the hub or axis of rotation.

The values of C_{l_r}, determined at various stations between the axis of rotation and the rotor blade tip, are substituted into equation (50) which is the differential form of equation (36).

$$dC_T = \frac{\sigma_r}{2}\left[\left(\frac{\lambda R}{r}\right)^2 + 1\right]^{1/2} C_{l_r}\left(\frac{r}{R}\right)^3 d\left(\frac{r}{R}\right) \qquad (50)$$

where

dC_T = rotor thrust coefficient of air forces on an elemental rotor annulus

A curve of dC_T vs. (r/R) is plotted and upon graphical integration of this curve the value of the thrust coefficient, C_T, is determined.

Several different values of θ_r at the blade root are assumed and the same procedure of calculating C_T is followed through. The correct values of θ_r are the values at which the known thrust coefficient is equal to the integrated thrust coefficient. A cross plot is made of θ_r at the root and C_T from which θ_r is determined at the known value of C_T.

The procedure for the determination of the torque coefficient is similar to that of the thrust coefficient, except that in this case θ_r is known from the thrust solution. Equation (51) is used to calculate the values of dC_Q which are plotted against (r/R). This equation is the differential form of equation (47).

$$dC_Q = \frac{\sigma_r}{2}\left[\left(\frac{\lambda R}{r}\right)^2 + 1\right]^{1/2} C_{D_0}\left(\frac{r}{R}\right)^4 d\left(\frac{r}{R}\right) + \frac{\lambda}{4}\sigma_r\left[\left(\frac{\lambda R}{r}\right)^2 + 1\right]^{1/2} C_{l_r}\left(\frac{r}{R}\right)^3 d\left(\frac{r}{R}\right)$$

$$+ \frac{\sigma_r}{2}\left[\left(\frac{\lambda R}{r}\right)^2 + 1\right]^{1/2} C_{l_r}\left[\sqrt{\left(\frac{\lambda R}{2r}\right)^2 + \frac{k_1 \sigma_r C_{l_r}}{8}\left[\left(\frac{\lambda R}{r}\right)^2 + 1\right]^{1/2}}\right]\left(\frac{r}{R}\right)^4 d\left(\frac{r}{R}\right) \qquad (51)$$

where

dC_Q = rotor torque coefficient about the axis of rotation of air forces on an elemental annulus

The first term of equation (51) contains a profile drag coefficient, C_{D_0}. Values of C_{D_0} for the corresponding values of C_{l_r} at a given value of (r/R) can be obtained from the rotor blade airfoil profile drag polor. The profile drag polor used in this paper was obtained from experimental data[7] (see Figure (7)). The profile drag coefficient is usually based on the value of the Reynold's Number at the 3/4 radius which is a weighted average value for the blade.

Graphical integration of the curve of dC_Q vs. (r/R) yields the torque coefficient.

---

[7]Montgomery Knight and Ralph A. Hefner, Static Thrust Analysis of the Lifting Airscrew, (U. S. National Advisory Committee for Aeronautics, Technical Note No. 626, 1937), pp. 37-38

V Results and Discussion

From a report by Fagan[8] experimental data was obtained for a three-bladed rotor having a five foot diameter. The blades were untwisted and had a two inch constant chord with an N. A. C. A. 0015 airfoil section. The tests were conducted in a nine foot open jet wind tunnel.

The thrust and torque coefficients, the rates of vertical ascent, and the blade angles of the experimental results are shown in Tables (I, II, III, IV and V).

Calculations were made for the theoretical values of the thrust and torque coefficients using equations (50) and (51). The values, listed in Tables (VI, VII, VIII, IX and X), were plotted vs. the blade angles as shown in Figures (8) and (9) and against each other as shown in Figure (10). On these curves the experimental values are shown as points. A table of sample calculations for the theoretical values of C_T and C_Q of the rotor model is shown in the appendix.

For low rates of vertical ascent the theoretical thrust and torque coefficients are in close agreement with the experimental values. The plot of C_T vs. C_Q for both the theoretical and experimental values indicates that for a given value of C_T the theory predicts too small a value of C_Q.

For greater rates of vertical ascent and blade angles the theoretical thrust coefficients are progressively higher while the theoretical torque coefficients are about the same value as the experimental for the whole range.

---

[8] Fagan, op. cit.

VI Conclusions

(1) This general theory predicts the thrust and torque on rotors having constant chord untwisted blades with good accuracy for hovering flight and small rates of vertical ascent. Further study should be made of agreement of this theory with experimental data for the cases of rotors having twisted and tapered blades.

(2) Better correlation of the experimental and theoretical thrust and torque coefficients can be obtained by the selection of another viscosity correction factor curve. The values of k, should be increasingly greater for the larger values of λ_v .

(3) An investigation should be made concerning the validity of assuming that the thrust and torque coefficient curves can be faired through the vortex ring area.

BIBLIOGRAPHY

Durand, W. F., Aerodynamic Theory, Berlin: Julius Springer, 1935. Vol. III, p. 162.

_____, Aerodynamic Theory, Berlin: Julius Springer, 1935. Vol. IV, pp. 230 and 350.

Fagan, Robert H., Vertical Ascent Analysis of the Lifting Airscrew, Unpublished Master's thesis, Georgia School of Technology, 1940. 27 pp.

Glauert, Herman, On the Vertical Ascent of a Helicopter, Aeronautical Research Committee Reports and Memoranda, No. 1132, 1927. p. 360.

Knight, Montgomery, and Hefner, Ralph A., Static Thrust Analysis of the Lifting Airscrew, U. S. National Advisory Committee for Aeronautics, Technical Note No. 626, 1937. pp. 37-38.

Rankine, W. J. M., On the Mechanical Principles of the Action of Propellers, Trans. Inst. Naval Architects, 1865. p. 13.

APPENDIX

As an example of the calculations for the theoretical thrust and torque coefficient values, the condition of the untwisted constant chord rotor in Fagan's paper with a blade angle, $\theta_r = 4^\circ$ and a rate of vertical ascent, $\lambda = .03$ was selected. As shown in Table II the experimental values of C_T and C_Q are .000636 and .00013, respectively, for the above condition. The procedure for the thrust and torque coefficient calculations is shown in Table XI.

As a first approximation, it is assumed that the theoretical value of C_T is equal to the experimental value so that a value of λ_v can be obtained. It was later found that the resulting value of C_T was greater than that first assumed, so another value of C_T between the previous two values was chosen and a new value of C_T calculated. In calculating the theoretical values for this paper it was found that although second and third approximate values of C_T to insert in equation (49) were assumed, the first integrated value was very near the integrated values for the second or third approximation.

From equation (49) the value of λ_v is calculated as

$$\lambda_v = \frac{\lambda}{\sqrt{\frac{C_T}{2}}} = \frac{.03}{\sqrt{\frac{.000636}{2}}} = 1.685$$

and

$k_1 = 1.1$ from Figure (6).

An explanation of Table XI is as follows:

Column (1): Stations of (r/R) are selected between the axis of rotation and the tip of the rotor blade.

Column (2): The rotor solidity at each station is calculated from the

equation

$$\sigma_r = \frac{bC_r}{\pi r} = \frac{3(2/12)}{\pi r} = \frac{1}{2\pi r}$$

Column (3): The values of σ_r for each station are multiplied by the factor $k_1 = 1.1$.

Column (4): λ is multiplied by the reciprocal values of column (1).

Column (5): The values of C_{lr}/a_o are obtained from Figures (4) and (5) which are plots of equation (30) for positive and negative values of C_{lr} respectively. For each station a value of C_{lr}/B is assumed. With the corresponding value of $k_1 \sigma_r$ from column (3) the value of $k_1 \sigma_r C_{lr}/B$ is determined from either Figure (4) or (5). The value of $\lambda R/r$ in column (4) is used to determine the value of ϕ . With ϕ and the known value of θ_r , C_{lr}/a_o is obtained. The slanting lines in the lower right quadrant of Figures (4) and (5) connect equal values of C_{lr}. This value of C_{lr} should correspond to the assumed value. Different values of C_{lr}/B for each station are assumed and the same procedure is followed until the final value of C_{lr}, as determined from the graph, is equal to that value assumed. This is a graphical trial and error solution of equation (30). No solution of equation (30) is obtained from the graphs for stations r/R 0.1 and 0.2 which indicates that the radical term of the equation is imaginary and also the presence of a vortex ring in the flow starting somewhere between stations r/R = 0.2 and 0.3.

Column (6): The values of C_{lr}/a_o in column (5) are multiplied by the slope of the lift curve, a_o, which is 2π/radian as stated on page (16) of this paper.

Column (7): The drag coefficients are obtained from the plot of C_{D_o} vs.

C_{lr}/a_o shown in Figure (7).

Column (8): dC_T is calculated from equation (50) for each station.

Column (9): dC_Q is calculated from equation (51) for each station.

The values of dC_T and dC_Q are plotted vs. (r/R) in Figures (11) and (12) respectively. The curves are faired from the values of dC_T and dC_Q at station (r/R) = 0.3 to zero at (r/R) = 0.

Graphical integration of these curves yields the theoretical values of C_T and C_Q.

Table I

Experimental Thrust and Torque Coefficient Values

$\lambda = 0$

θ	C_T	C_Q
2	0.0005125	0.000103
4	0.00149	0.0001495
6	0.002735	0.000237
8	0.00417	0.000367
10	0.00563	0.0005225
12	0.00685	0.000678

Table II

Experimental Thrust and Torque Coefficient Values

$\lambda = .03$

θ	C_T	C_Q
4	0.000636	0.000130
6	0.001815	0.000238
8	0.003188	0.000344
10	0.004675	0.000511
12	0.00604	0.000685

Table III

Experimental Thrust and Torque Coefficient Values

$\lambda = .06$

θ	C_T	C_Q
6	0.000522	0.0001798
8	0.001688	0.0002575
10	0.00315	0.000456
12	0.00477	0.000661

Table IV

Experimental Thrust and Torque Coefficient Values

$\lambda = .09$

θ	C_T	C_Q
10	0.001355	0.00031
12	0.00302	0.0005425

Table V

Experimental Thrust and Torque Coefficient Values

$\lambda = .12$

θ	C_T	C_Q
12	0.0009525	0.000330

Table VI

Theoretical Thrust and Torque

Coefficient Values

$\lambda = 0$

θ	C_T	C_Q
2	0.000557	0.000102
4	0.001544	0.000148
6	0.00275	0.000235
8	0.00409	0.000358
10	0.00555	0.000527
12	0.00710	0.000714

Table VII

Theoretical Thrust and Torque

Coefficient Values

$\lambda = .03$

θ	C_T	C_Q
4	0.00076	0.000125
6	0.00194	0.000211
8	0.00331	0.000336
10	0.00478	0.000498
12	0.00628	0.000684

Table VIII

Theoretical Thrust and Torque

Coefficient Values

$\lambda = .06$

θ	C_T	C_Q
6	0.00067	0.000148
8	0.00200	0.000276
10	0.00360	0.000451
12	0.00518	0.000652

Table IX

Theoretical Thrust and Torque

Coefficient Values

$\lambda = .09$

θ	C_T	C_Q
10	0.00200	0.000338
12	0.00351	0.000539

Table X

Theoretical Thrust and Torque

Coefficient Values

$\lambda = .12$

θ	C_T	C_Q
12	0.00160	0.000357

Table XI

Calculation of C_T and C_Q

$\theta = 4^\circ$ $\lambda = .03$

Three-bladed Rotor Constant Chord, $C_r = 2"$

1	2	3	4	5	6	7	8	9
r/R	σ_r	$k_1 \sigma_r$	$\lambda R/r$	C_{lr}/a_o	C_{lr}	C_{D_o}	dC_T	dC_Q
.1	.636	.70	.30					
.2	.318	.35	.15					
.3	.212	.233	.10	-.0100	-.0628	.0113	-.000181	.000005626
.4	.159	.175	.075	-.0019	-.01192	.0113	-.0000606	.00002127
.5	.1273	.14	.06	.003	.01885	.0113	.00015	.0000498
.6	.106	.1166	.05	.0075	.0471	.0113	.00054	.0000975
.7	.091	.100	.0428	.0115	.0722	.0113	.001129	.0001697
.8	.0795	.0875	.0375	.015	.0941	.0113	.001911	.0002694
.9	.0707	.0778	.0333	.0175	.1100	.0113	.002832	.0003981
1.0	.0636	.070	.03	.0190	.1194	.0114	.0038	.0005513

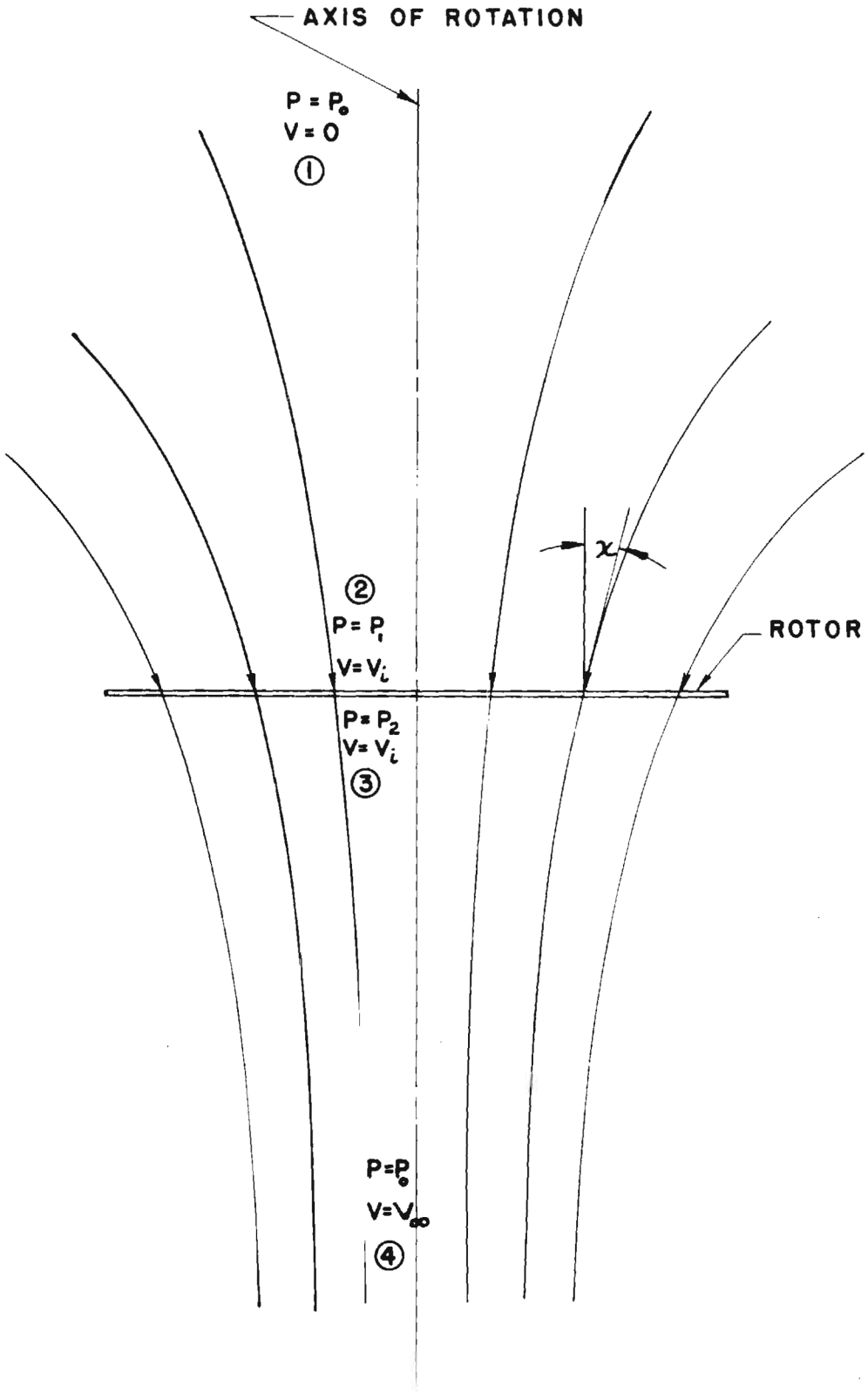

FIGURE 1

VELOCITIES WITH RESPECT TO FIXED COORDINATES

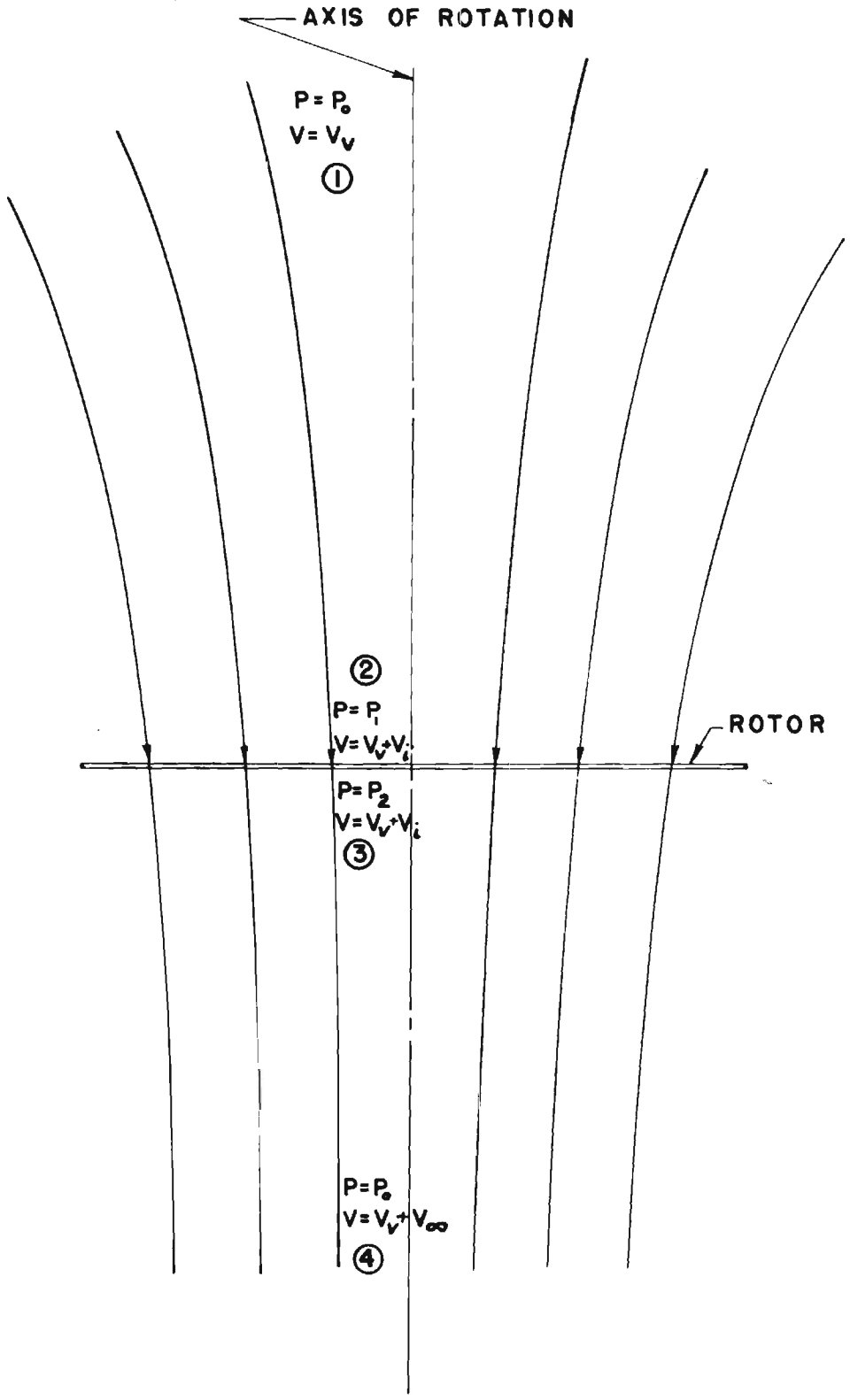

FIGURE 2

VELOCITIES WITH RESPECT TO THE ROTOR

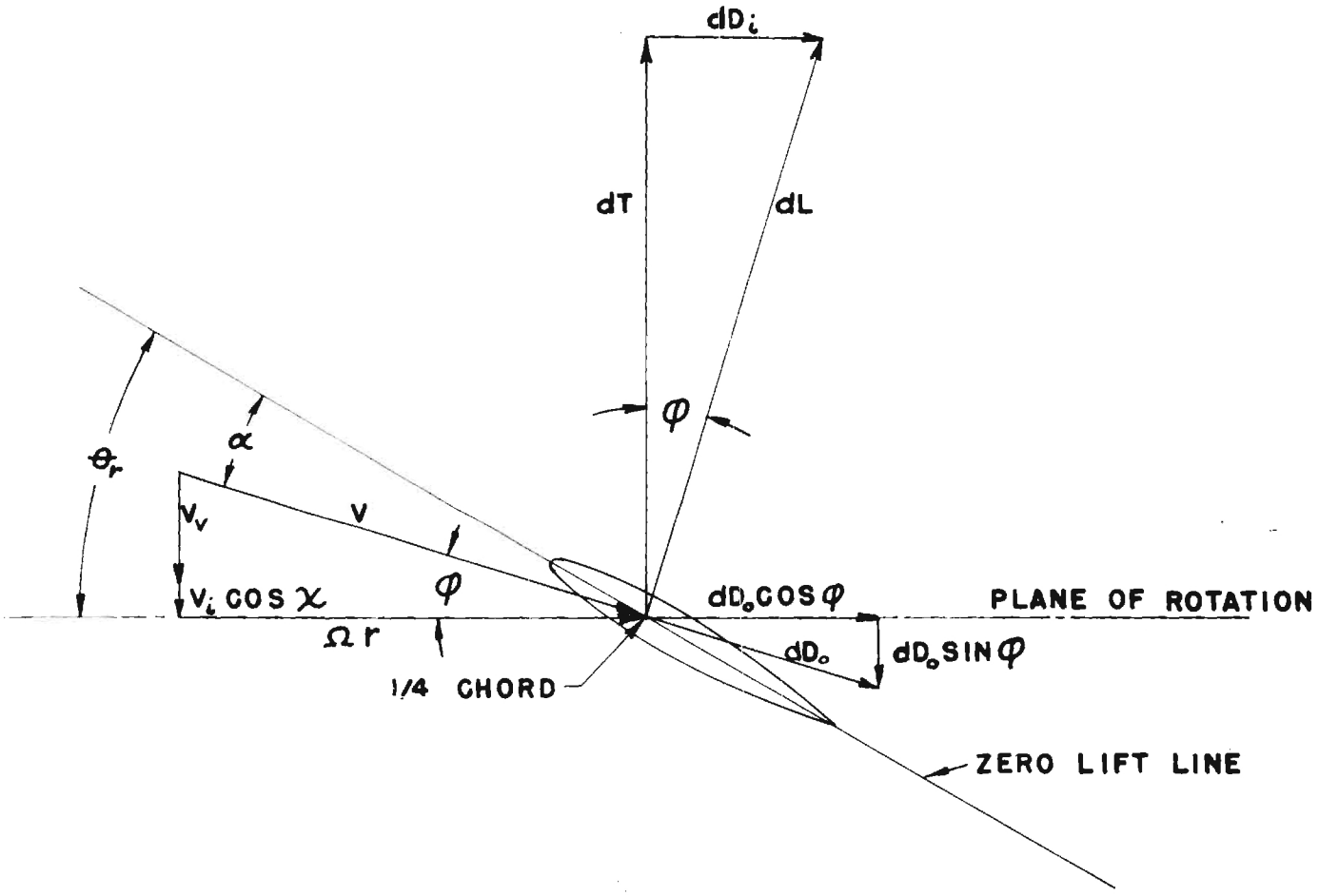

FIGURE 3

VELOCITIES, ANGLES, AND FORCES

AT A BLADE ELEMENT

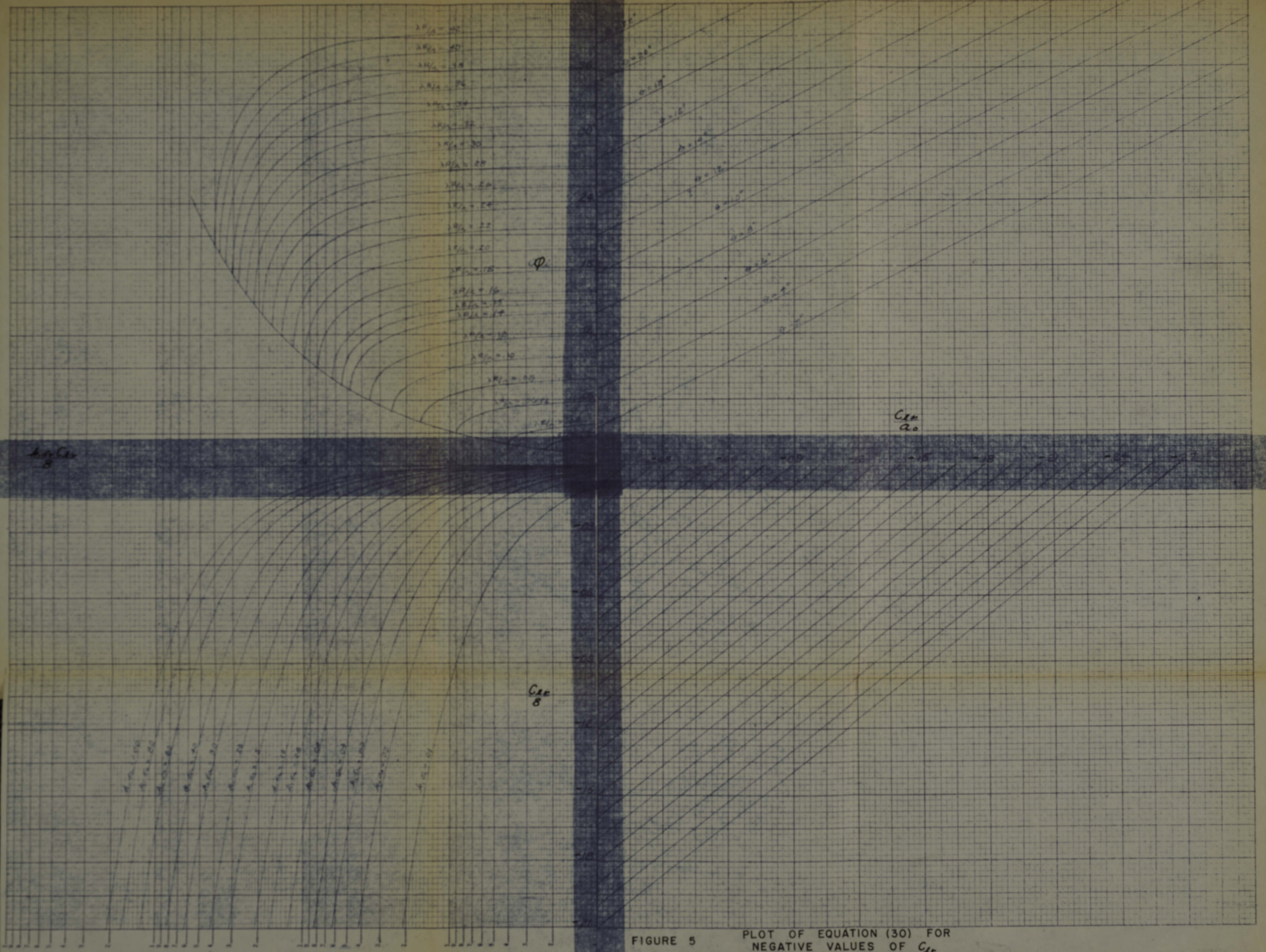

FIGURE 5 PLOT OF EQUATION (30) FOR NEGATIVE VALUES OF C_{lr}

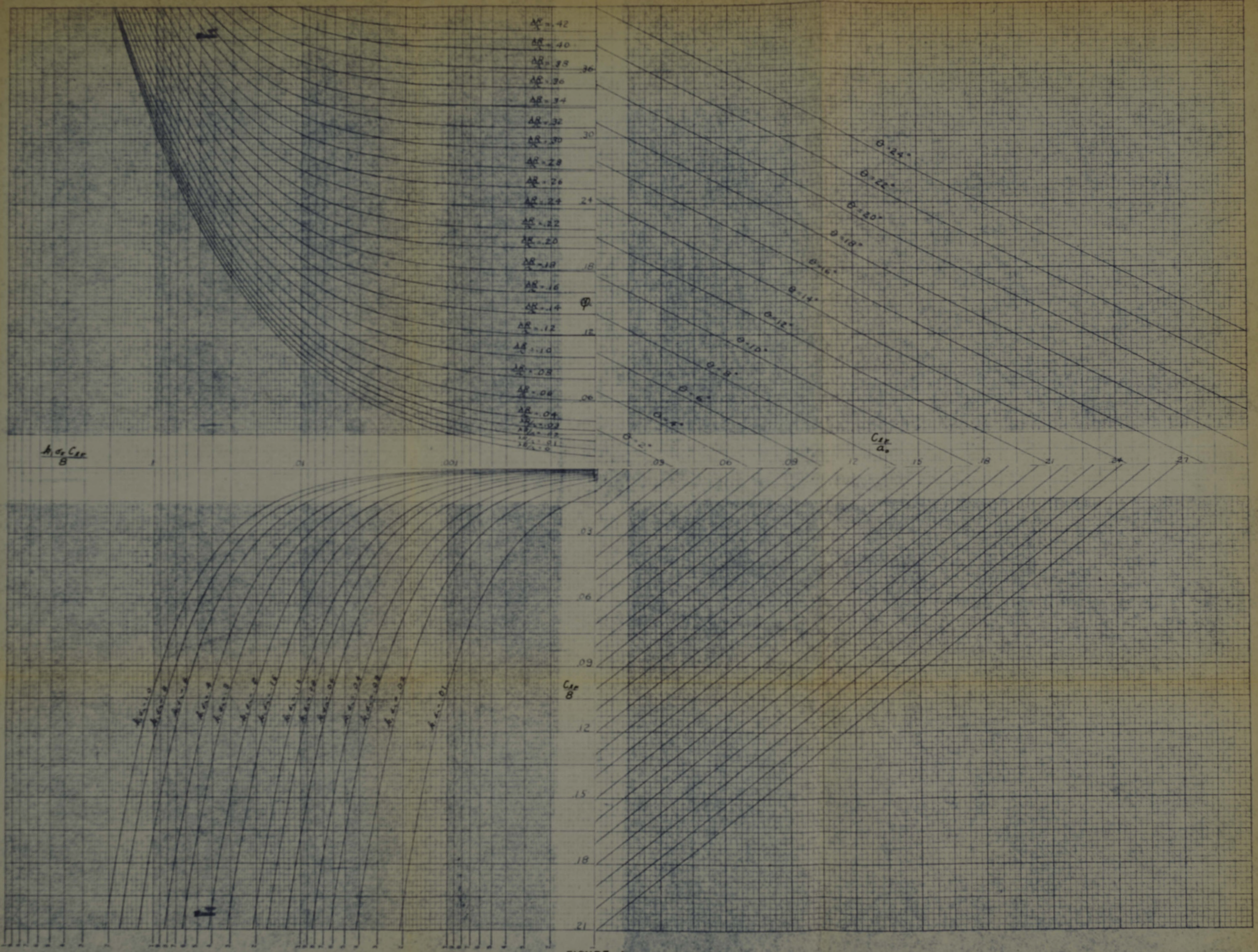

FIGURE 4
PLOT OF EQUATION (30)
FOR POSITIVE VALUES OF C_{Lr}

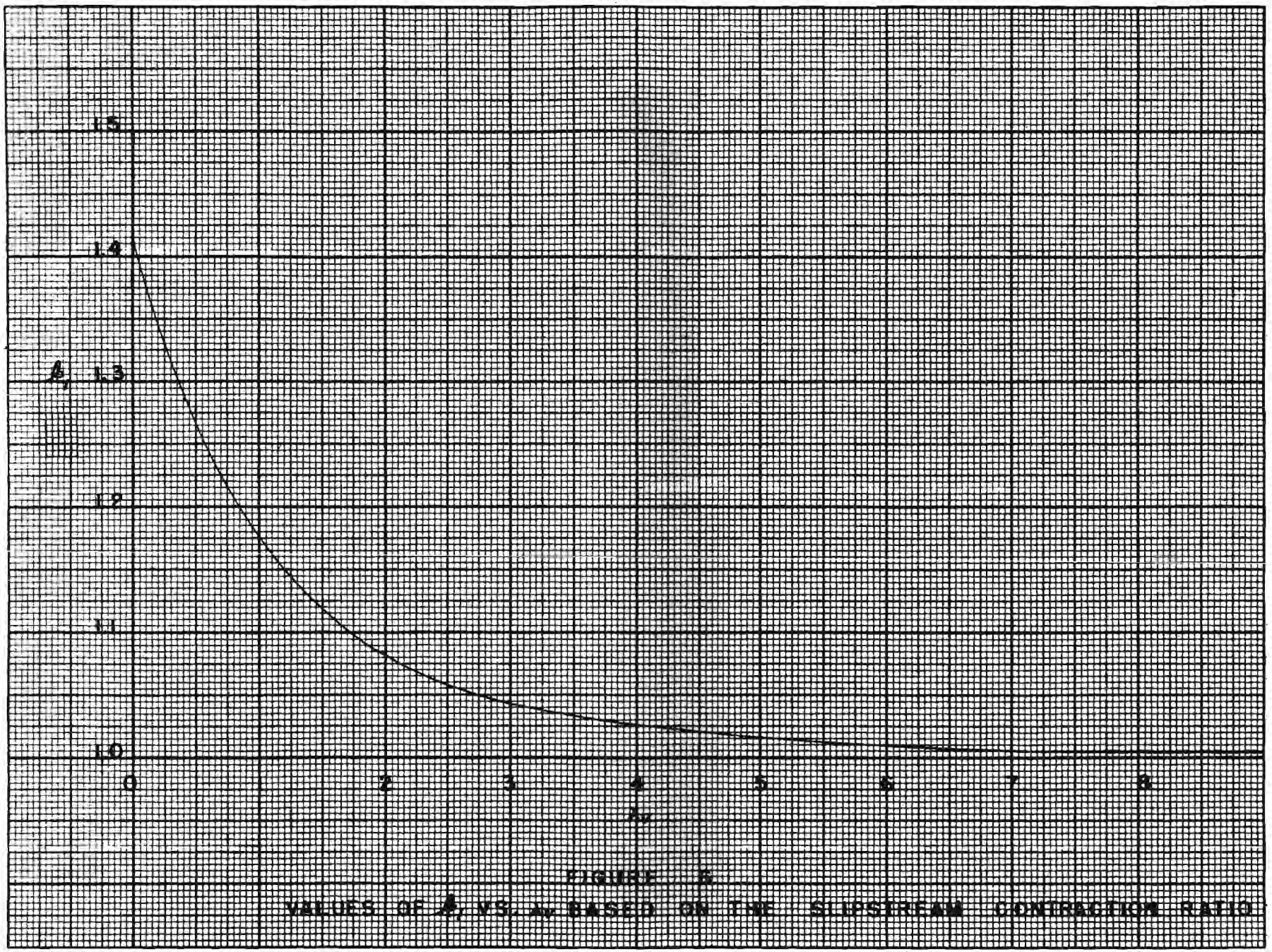

FIGURE 5

VALUES OF ϕ_f VS. λ_w BASED ON THE SLIPSTREAM CONTRACTION RATIO

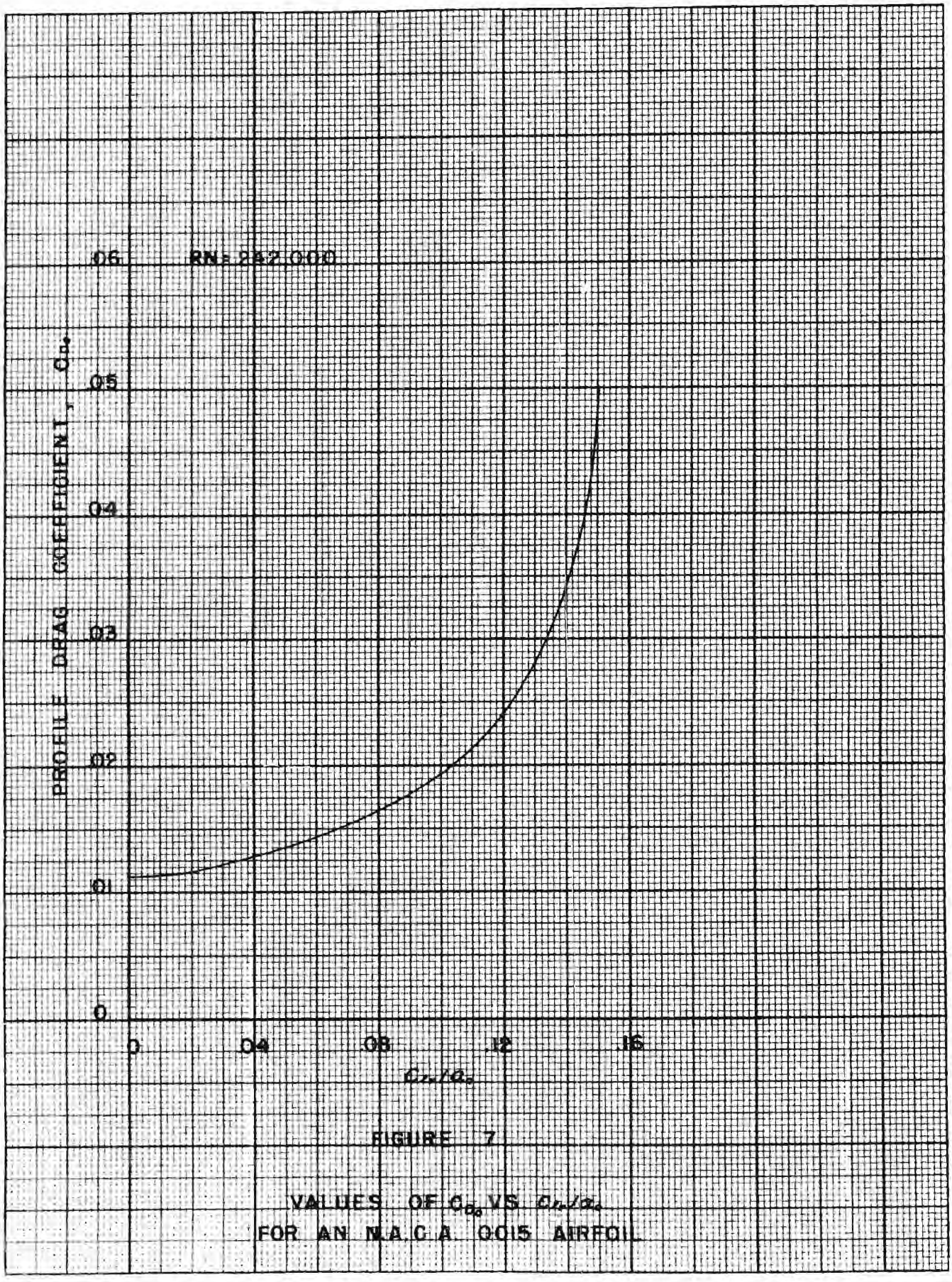

FIGURE 7

VALUES OF C_{d_o} VS $C_{l_{max}}/a_o$
FOR AN N.A.C.A. 0015 AIRFOIL

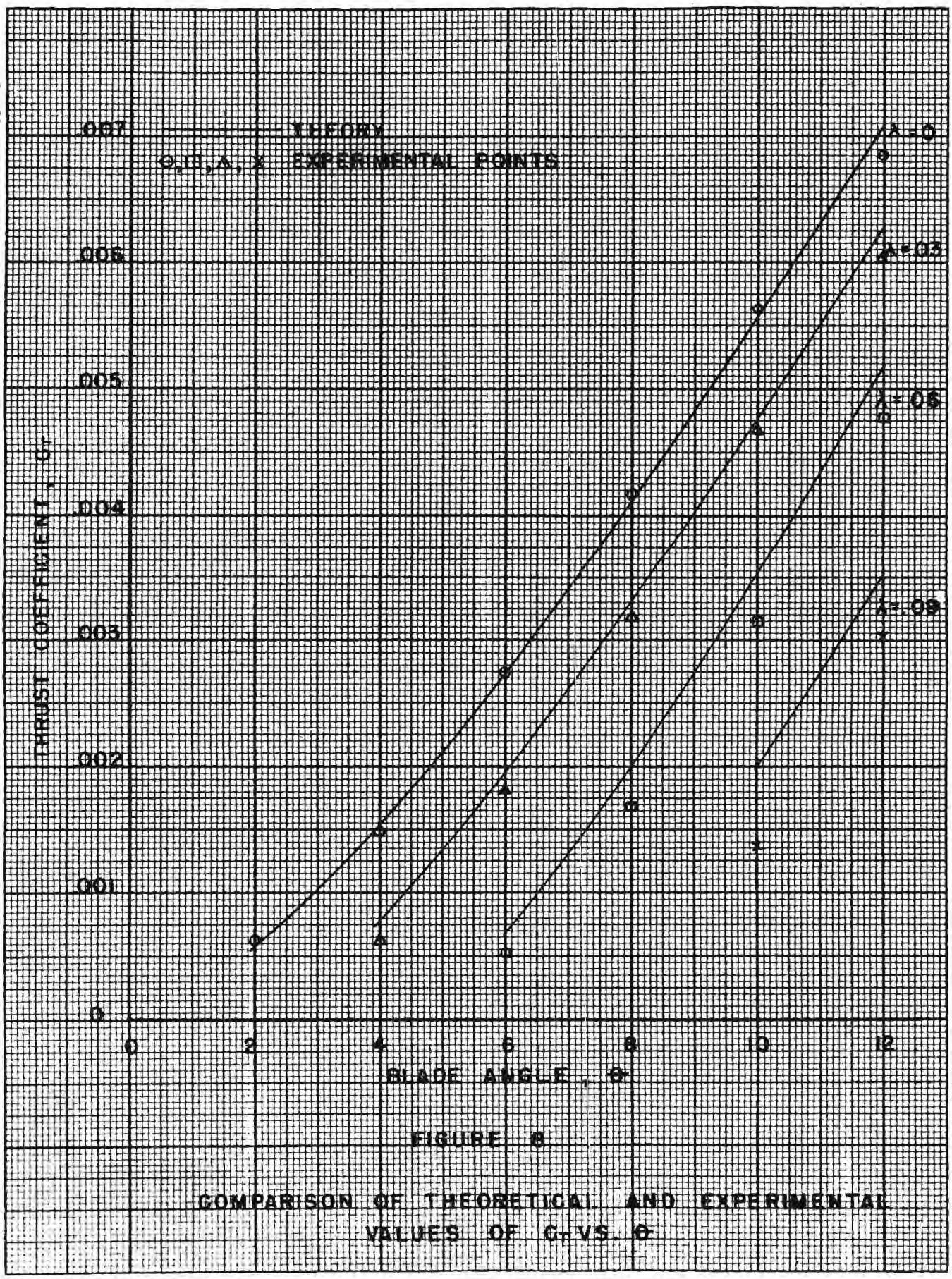

FIGURE 8

COMPARISON OF THEORETICAL AND EXPERIMENTAL VALUES OF C_T VS. θ

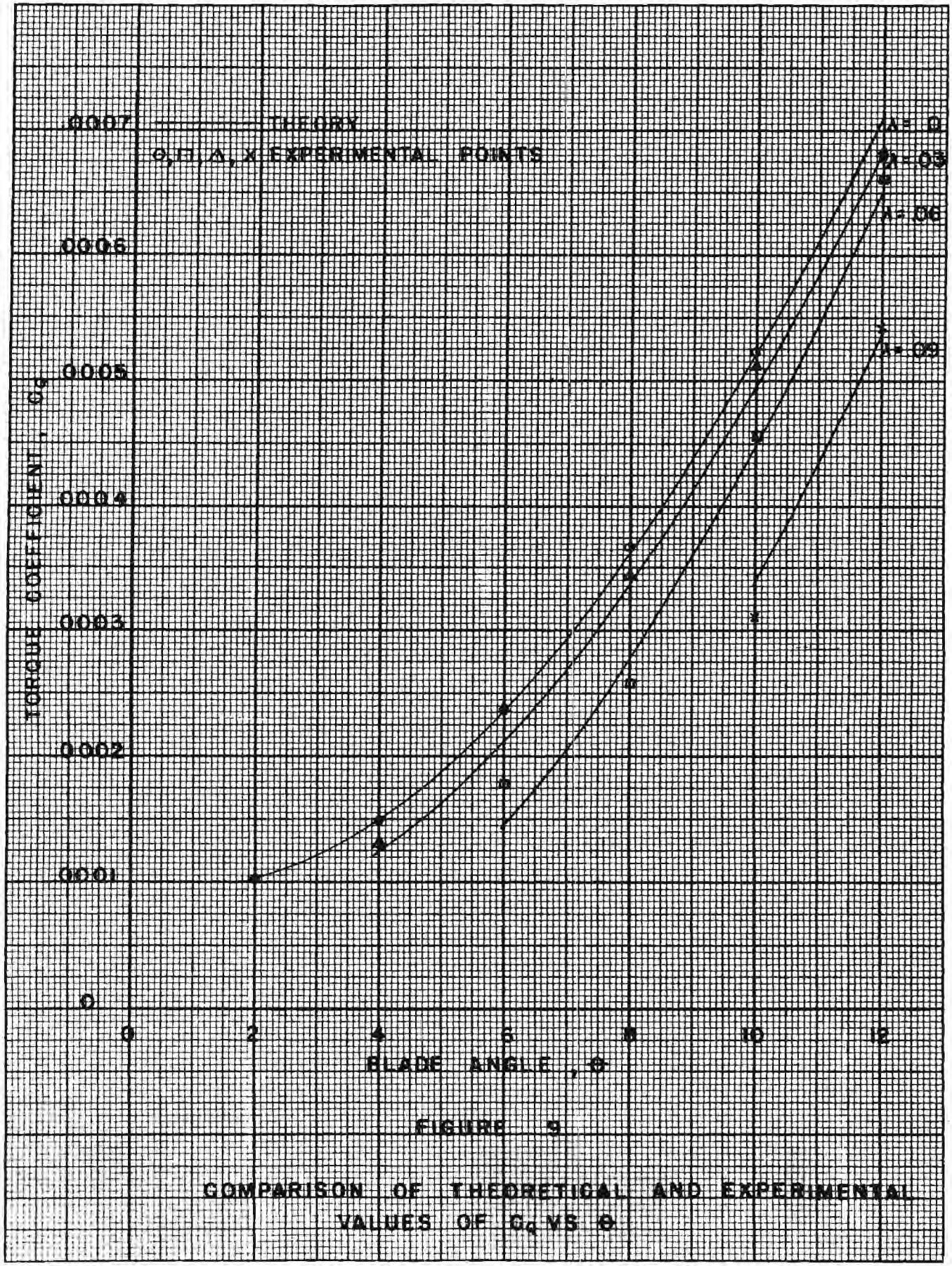

FIGURE 9

COMPARISON OF THEORETICAL AND EXPERIMENTAL VALUES OF C_Q VS Θ

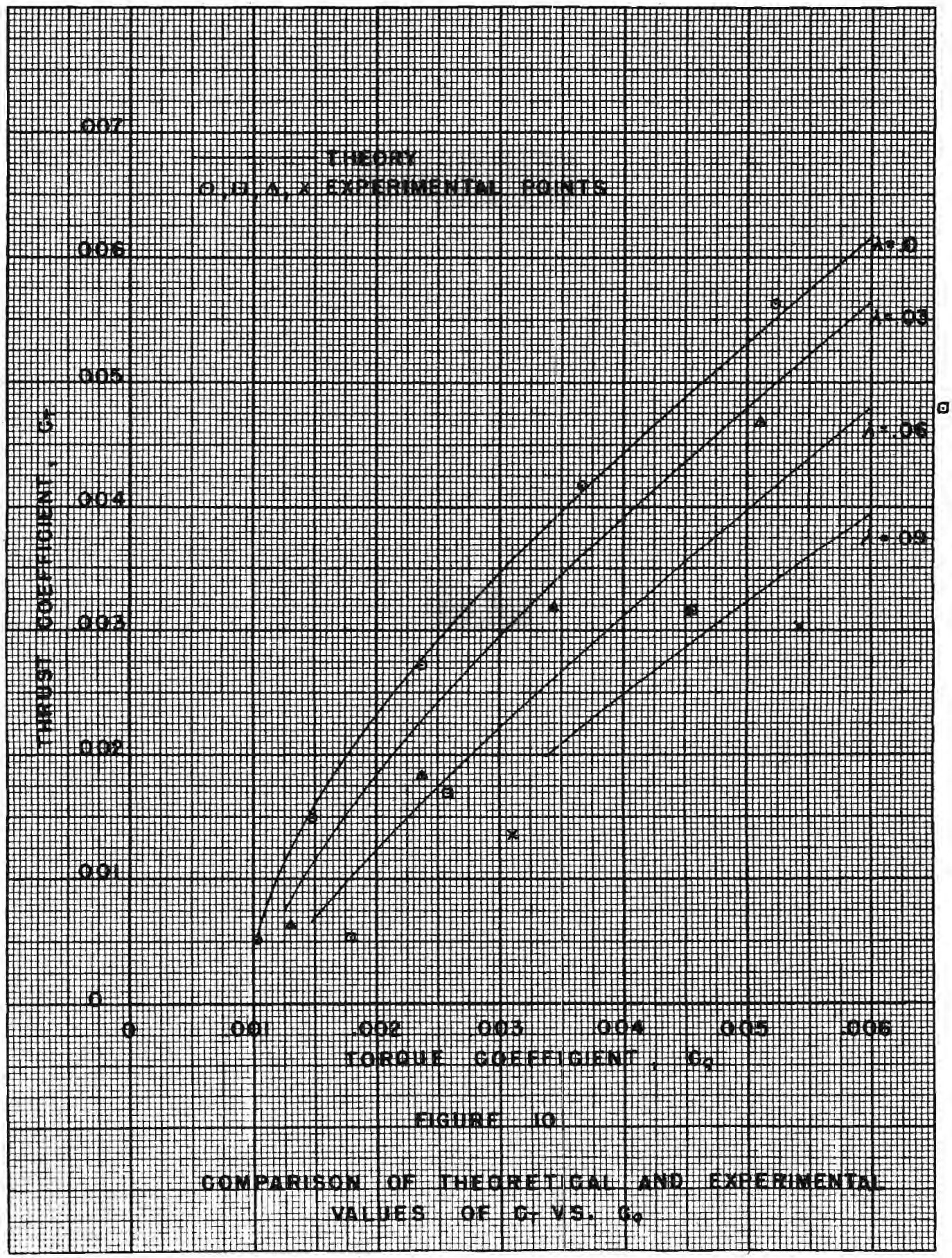

FIGURE 10

COMPARISON OF THEORETICAL AND EXPERIMENTAL VALUES OF C_T VS. C_Q

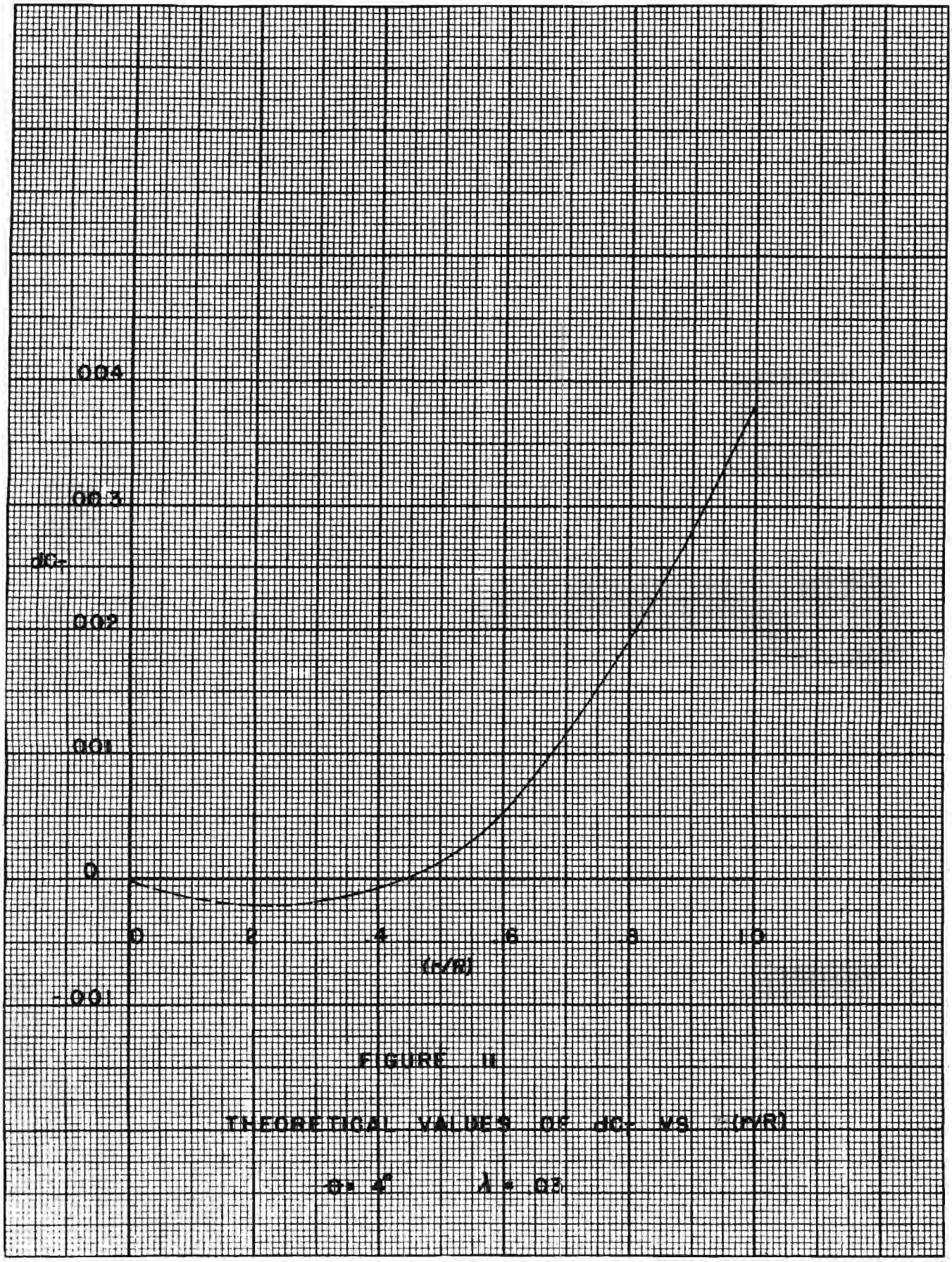

FIGURE II

THEORETICAL VALUES OF dC_r VS (r/R)

$\Theta = 4^\circ$ $\lambda = .03$

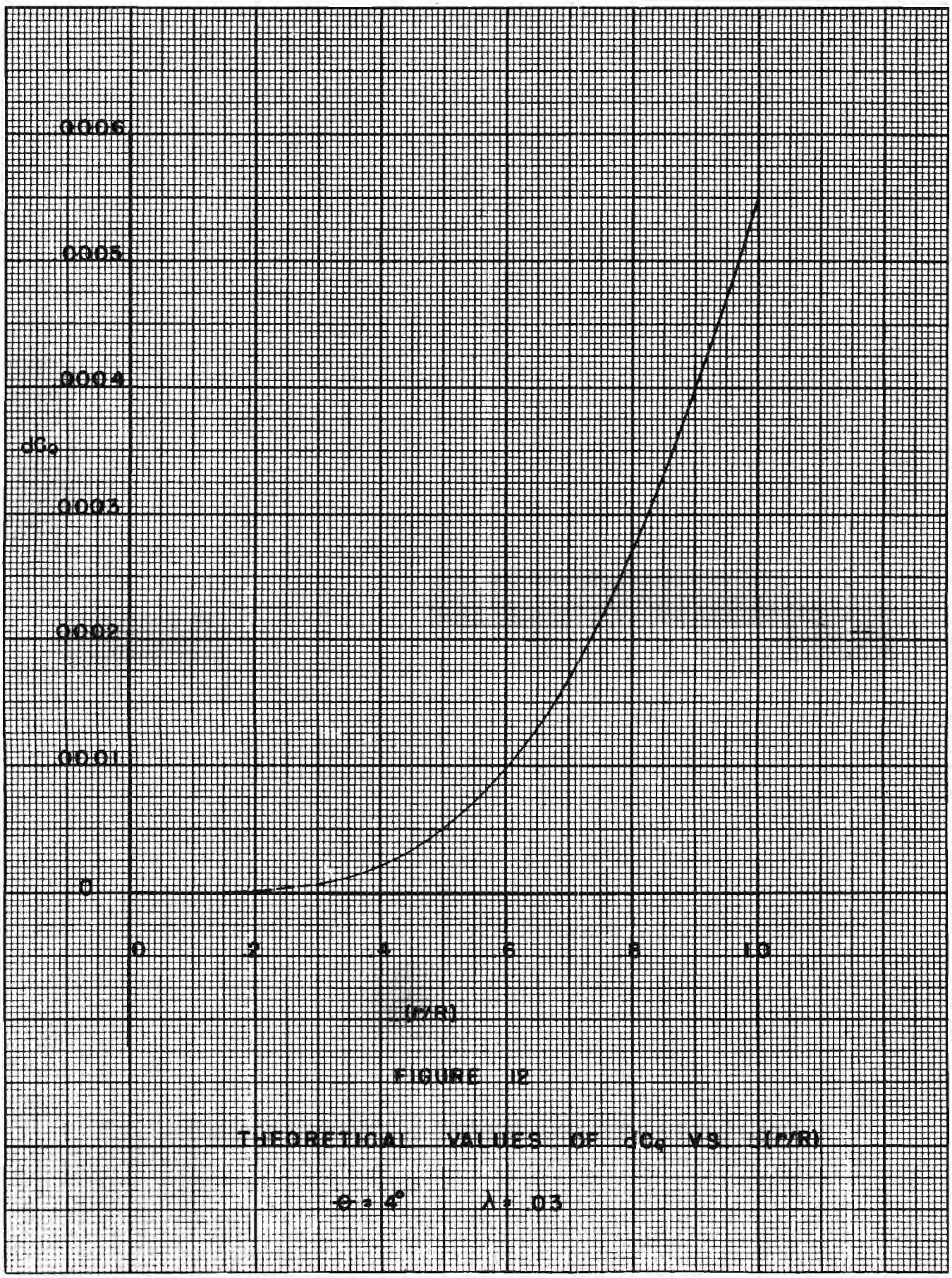

FIGURE 12

THEORETICAL VALUES OF dC_0 VS. (r/R)

$\Theta = 4^\circ$ $\lambda = .03$